Adsorption of Molybdenum from Wastewater by Surface Altered Agricultural Solid Waste

Maria Joseph, Vinolia Thamilarasi
Department of Chemistry, KPR Institute of Engineering and Technology, Coimbatore-641407, INDIA

Molagoundampalayam Venkatachalam, Sureshkumar*+
Department of Chemistry, Jansons Institute of Technology, Coimbatore-641659, INDIA

Arun Kumar, Priya
Department of Civil Engineering, KPR Institute of Engineering and Technology, Coimbatore-641407, INDIA

ABSTRACT: *The palm fruit husk, an agricultural solid waste does not adsorb Mo(VI). The intent of this endeavor was to estimate the adsorption capacity of the SAPFH towards Mo (VI) in wastewater. Hence the surface was altered using a surface activating group, cetyl trimethyl ammonium bromide (CTAB). The husk of the palm fruit, whose surface was modified, was subjected to evaluate the extent of extracting molybdenum that is present in an aqueous solution. The maximal removal of molybdenum occurs at pH 2.0. The adsorbent dose necessary for the maximum adsorption of MoO_4^{2-} was lesser for wastewater than for pure aqueous solutions. MoO_4^{2-} took a long time to attain equilibrium at high concentrations. The stability results were suited to Langmuir, Freundlich, and Dubinin-Raduskevich adsorption isotherms models. Dynamic investigation revealed that the uptake obeyed pseudo-second-order kinetic effigy. The adsorption of adsorbates did not change significantly with an increase in temperature. Desorption of Mo (VI) showed that it is possible to retrieve Mo (VI) from the spent adsorbent. The influence of accompanying negative ions such as chloride, phosphate, sulfate, and chromate on the Mo (VI) uptake was explored and the anions compete with Mo(VI) ions.*

KEYWORDS: *Palm fruit husk; Cetyl trimethyl ammonium bromide; Molybdenum (VI); Isotherms.*

INTRODUCTION

Molybdenum is one of the biologically active transition elements and is a trace mineral that is important for the development and maturation of many living organisms [1]. Molybdenum is normally utilized as a supplement in special steel and lubricant [2,3], die casting, pigments for printing inks, solid lubricants, and aircraft paints [4]. Mo is also used in industries like iron, steel, electrical, chemical, fertilizer and in alloys, colors, catalysts, etc. [5]. The permitted limit of molybdenum in consuming water recommended by the WHO is 70μg/L. The permissible limit 340 μg/L for surface water was implemented as standard quality in Flanders in the year 2011 January by the European Water Framework Directive (2000/60/EC). Hence the concentration of Mo in the wastewater discharge

should not overcome this value. Mo is usually present as oxyanion in wastewater [6] and the predominant form is molybdate anion, MoO_4^{2-} [2].

The intake of high concentrations of molybdenum-contaminated water results in limb weakness, headache, kidney damage, deformities in some animals, chlorosis, yellowing of leaves in plants [7, 8], and molybdenosa disease [9, 10].

Several techniques have been employed to remove molybdenum and a few of them are discussed as follows: Orrego et al used an ion exchange process to recover molybdenum from copper leaching solutions [11]. Mo(VI) and W(VI) were isolated from HCl by employing cyanex-923 by solvent extraction [12]. The solvent extraction method was adapted to reclaim molybdenum from the sulfur-removed spent catalyst by Pradhan et al. [13]. The efficiency of removing molybdenum from the water was investigated by *Zhang et al* by using $FeCl_3$ [14]. *Sabullah et al* used a bioremediation technique to assess Enterobacter sp. Strain saw – 1 on Molybdenum [15]. The strong anionic resin was used to separate Mo and Vanadium from the synthetic sulphuric acid solution [16]. *Velizarov et al.* observed that ultrafiltration and microfiltration methods were not able to remove inorganic anions such as CrO_4^{2-}, MoO_4^{2-}, VO_3^-, SCN^-, SO_4^{2-}, and PO_4^{3-} from the solution directly [17]. Yobilishetty and Marathe removed Mo from streams of wastewater by using a micellar-enhanced ultrafiltration method by employing anionic, non-ionic, and mixed surfactants [18]. To control pollution, several techniques have evolved with different degrees of success. A few of them are ion exchange, sedimentation, precipitation, electrolysis, coagulation, oxidation, filtration, adsorption, etc. which have their own limitations like less efficiency, sludge formation and disposal, and operating conditions.

Of all these methods, the adsorption process is better on par with other methods by virtue of its simple functioning and design. A few of the adsorbents used for the removal of molybdenum are discussed here. *Ferreira et al.* explained the Mo(VI) - calmagite complex uptake on activated carbon which is commercially available (Filtrasorb Co., USA) at pH 2 [19]. Molybdate and tetrathiomolybdate uptake by pyrite and goethite was maximal at pH of less than 7 [20]. *Afkhami* and *Norooz-Asl* used maghemite nanoparticles for the molybdenum uptake from water [21]. Goldberg explored the removal of molybdenum by Gibbsite in the proximity of phosphorus or sulfur [22]. Pennesi et al. researched the Posidonia oceanica (Tracheophyta) Biomass for the adsorption of Vanadium (III) and Molybdenum (V) from Wastewater [23]. *Johansson et al.* explored the use of modified algal-based biochars for the biosorption of molybdenum [24]. Strong and weak ion exchange resins were employed to remove molybdenum and vanadium [25]. Lian et al used nano-zero valent iron to remove Mo (VI) from aqueous solutions [26]. Several adsorbents like mesoporous aluminum oxides [27], NaOCl- oxidized multi-walled CNT [28], alumina [29], silica-based hydroxyoxime [30], calcined wheat bran [31], Chitosan [32], chitosan nanoparticle [33] were used to investigate the adsorption of Molybdenum. The acute Mo (VI) adsorption on thermally treated and acid-activated residues from treatment plants of drinking water was also reported [34].

Nowadays agricultural waste materials like mangosteen fruit shell [35], and kenaf fiber [36] are used as effective adsorbents, as a result of reasonable rate, high performance, availability, regeneration ability, and metal recovery, for ion removal [37]. Therefore surface modification may also be carried out to lignocellulosic material such as palm fruit husk, which is obtained from the palmyra tree (Borassus Flabellifer).

The intent of this endeavor was to estimate the adsorption capacity of the SAPFH towards Mo (VI) in wastewater. The impact of association moment, adsorbent quantity, pH, and thermal reading were investigated.

EXPERIMENTAL SECTION

Sodium molybdate of analytical quality was utilized in the preparation of solutions. Analytical quality chemicals were procured and used as reagents.

Synthesis and analysis of surface-altered palm fruit husk (SAPFH)

The collected waste PFH was seared, beaten, and strained to a grain size of 150-250 μm. Loading CTAB was done at different initial concentrations (0.2 to 2.0%). In order to prepare the adsorbent economically, 1 % CTAB was selected. The exterior alteration of the PFH was carried out by mixing and stirring 10 g of PFH and 1 % CTAB solution in 500 mL conical flask for about 5 hours at 250 rpm on an orbital shaker (Osi-26 Neolab). The liquid and palm fruit husk should be kept in the mixture without interruption. It was filtered. To disassociate the surface-adhered surfactant, the residue was scrubbed various times with distilled water and drained in a hot air kiln at 60 °C

for 7 hours. After that, the characterization studies were carried out using Physico-chemical methods and the characteristics are presented in Tables 1 and 2. The surface-altered PFH was weighed and shaken with 50 mL of water at different pH values over a span of 2 h to study the characteristics of surfactants. After 2 hrs, Whatman filter paper was used to separate the adsorbent and to disassociate the surface adhered surfactant, scrubbed various times with distilled water, drained in a hot air oven, and analyzed using CHN analyzer (Vario EL III, Germany).

Batch mode adsorption studies

0.50 g of SAPFH and 50 mL of various concentrations of molybdenum solution at an initial pH 2.0 were blended at 160 rpm at pH 2.0 and rotated at a high speed of 2500 rpm for 45 minutes. The concentration of molybdate ion that was not used was determined by spectrophotometric method with 1 % gallic acid and 1 % hydroxylamine using a UV-Visible spectrophotometer [38]. The complex formed had an absorption maximum at 420 nm in an acidic medium and Beer law conformed in the concentration extent from 3.02 to 25.12 mg/L of Molybdenum. 2.5 mL of gallic acid solution (1 % solution in 20 % ethanol) and 2.5 mL of 1 % hydroxylamine solution were added to a series of standard solutions. Absorbance was measured at 420 nm. The concentration of the Molybdate was determined by a plot between absorbance and the concentration of molybdenum. The quantity of Molybdenum uptake was evaluated from the change in the solution concentration before and later uptake. The pH impact on Molybdenum ion uptake was examined for the 40 and 80 mg/L solution concentrations. To determine the impact of contact time, the residual molybdenum ion concentration was computed by taking samples at definite time intervals. In this case, the phenol red method was employed to study the bromide desorption from the adsorbent surface [39]. The impact of adsorbent quantity for synthetic wastewater was assessed by changing the dosage from 50 to 1000 mg/50 mL for different dilutions of molybdenum ion, 20-100 mg/L. Adsorption isotherm models such as the Langmuir, Freundlich, and Dubinin-Radushkevich isotherms are employed to explain the results of uptake at equilibrium.

Batch mode desorption studies

The surface-altered PFH utilized to adsorb was detached from the solution and drained with water to take away the Mo (VI) that is not adsorbed. The eluted Mo (VI) was evaluated as previously by adding 0.05 g adsorbent loaded with Mo(VI) to the 50 mL of desorption solution at pH varying between 2.0 to11.0 and stirred for equilibrium time. The process is repeated for identical solutions and the mean values are recorded.

Influence of accompanying ions

The impact of different quantities of accompanying negative ions like Cr (VI), PO_4^{3-}, Cl^-, and SO_4^{2-} on the molybdenum uptake by SAPFH was examined.

Influence of Temperature

The impact of heat on the uptake of molybdenum ions is studied by stirring 0.20 g of adsorbent and various dilutions of molybdenum in a thermostatic stirrer at various temperatures such as 32 °C, 40 °C, 50 °C, and 60 °C.

RESULTS AND DISCUSSION
Characteristics of SAPFH

The proportion of the RPFH is 53.4% α- cellulose, as reported [40]. The surface of PFH was altered by a positive surface activating agent, cetyl trimethyl ammonium bromide (CTAB) to enhance the anion uptake [41]. A surfactant bilayer was formed between CTAB and functional moieties on the exterior of the palm fruit husk. It was noted that maximal piling up of 84.97 CTAB mg/g of PFH was achieved at an equilibrium concentration of 1.0 %. The outcome of the basic investigation of RPFH and SAPFH is specified in Table 1. The uptake of CTAB onto the exterior of palm fruit husk increases the percentage of Carbon, Hydrogen, and Nitrogen.

The uptake of CTAB on PFH lessens the surface area of the SAPFH (Table 2). Krishna et al. reported a similar decrease in BET surface area of surfactant-modified montmorillonite clay [42].

The zero point charge pH assay of untreated palm fruit husk (6.2) is elevated to 7.4 for SAPFH showing that the positive potential of the surface is by virtue of the synergy between the alkyl part of CTAB and palm fruit surface due to hydrophobic binding. This is evidenced by the increase in the overall percentage of basic moieties from 0.54 meq/g to 0.96 meq/g (Table 3).

The SEM images reveal the surface properties of the raw palm fruit husk as a macroporous irregular tubular

Table 1: Elemental composition of (a) Raw palm husk, (b) SAPFH and (c) SAPFH after leaching at different pH.

Material		% C	% H	% N
(a) Raw palm fruit husk		45.82	5.49	0.51
(b) SAPFH		51.24	6.11	0.95
(c) SAPFH after leaching at	(i) pH 2.0	51.21	6.14	0.93
	(ii) pH 7.0	51.23	6.09	0.94
	(iii) pH 11.0	51.26	6.13	0.96

Table 2: Characteristics of Raw Palm Fruit husk and SAPFH.

Parameter	Raw palm fruit husk	SAPFH
BET surface area (m^2/g)	20.64	18.6
pH$_{ZPC}$	6.2	7.4
pH (1% solution)	4.75	4.52
Conductivity (1% solution) (mS/cm)	0.38	0.17
Bulk density (g/mL)	0.16	0.20
Iodine number (mg/g)	4.87	2.538
Ion exchange capacity (meq/g)	0.15	0.3
Mechanical Moisture content (%)	11.48	10.06
Specific gravity	0.362	0.437
Porosity (%)	51.28	53.13
Ash content (%)	3.85	2.11
Ash analysis:		
Sodium (%)	13.8	13.71
Potassium (%)	0.68	0.65
Calcium (%)	1.65	1.67
Phosphorous (%)	0.0021	0.0015
Iron (%)	4.38	5.02

Table 3: Surface functional groups.

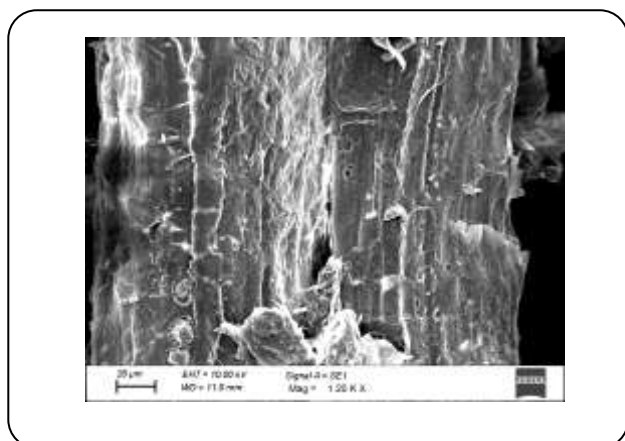| Surface functional groups	Carboxylic (meq/g)	Lactones (meq/g)	Phenolic (meq/g)	Total (meq/g)	Basic (meq/g)	Total capacity
Raw palm fruit husk	4.25	0.30	2.98	7.53	0.54	8.07
	(56.44 %)	(3.98 %)	(39.57 %)	(100 %)	(6.69 %)	-
SAPFH	5.38	0.22	1.524	7.124	0.96	8.084
	(75.519 %)	(3.088 %)	(21.39 %)	(100 %)	(11.87 %)	-

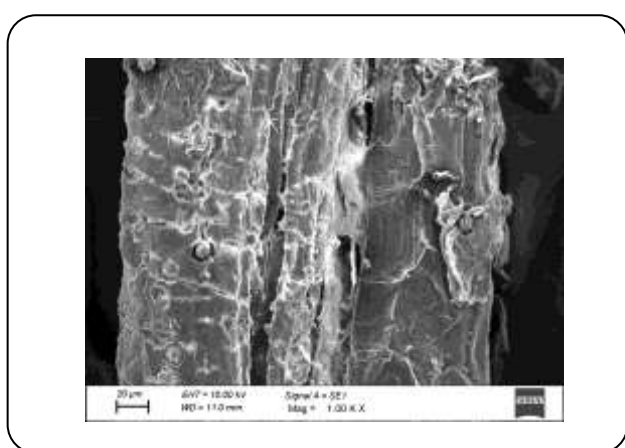**Fig. 1: SEM Micrograph of Raw Palm Fruit Husk (PFH).**
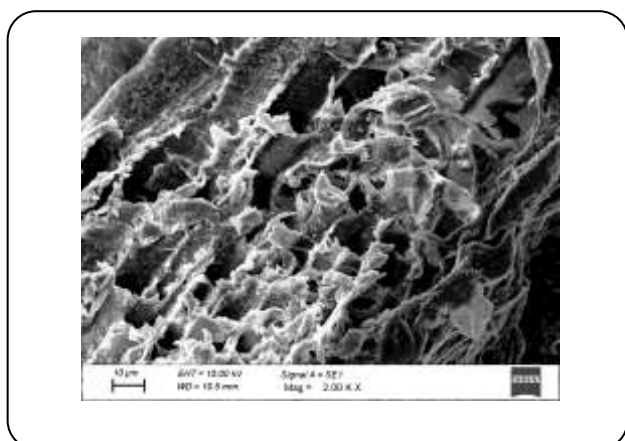

Fig. 2: SEM Micrograph of SAPFH.

Fig. 3: SEM Micrograph of molybdate loaded SAPFH.

structure (Fig. 1 and Fig. 2). SAPFH SEM micrography showed a shrink in the number of the orifice. The BET surface area of SAPFH is smaller than the unaltered palm fruit husk. By virtue of the adhesion of the surface active moieties to the surface of the inherent structure, the pore

channel narrows. Mo-loaded SAPFH SEM micrograph is shown in Fig. 3. It was observed that there were morphological changes due to the clogging of the adsorbed pores. *Arami et al* recorded identical results for the uptake of acid dyes onto orange peel [43].

Impact of pH on Adsorption and Desorption

pH is a salient variable in the adsorption phenomenon. The pH_{zpc} of SAPFH was 7.4. If the count of protonated surface moieties is greater than that of the dissociated group, it is suitable for anion adsorption. A state for zero point charge (pH_{zpc}) is attained when an equal number of both types of groups is present [44]. Since pH_{ZPC} for SAPFH is 7.4, the anion adsorption is highly favored in the pH limit of 2.0 to 7.4.

At the initial pH 2.0, the removal of Mo(VI) species was 93 %, and a further increase in pH to 11.0, decreased the removal to 1.7 % for the initial Molybdenum ion concentration of 40 mg/L (Fig. 4). The reduction in removal is by virtue of decrease in protonation and the OH^- ions participate in the competition to the site of adsorption. Similar pH dependence for the Mo(VI) uptake on Tamarindous Indica [9], sugarcane bagasse ash [45], goethite [20], ferrihydrite [46], and pyrite [47] was also reported.

The percent desorption of Mo(VI) shoots up from 0.4 to 78 % (Fig. 4) as the pH in desorption raised from 2.0 – 11.0. The movement of Mo(VI) moieties from the site of adsorbent by hydroxide ions causes the desorption of Mo(VI), specifying that the uptake occurs mainly through an ion exchange mechanism or by a weak force of attraction between the Mo(VI) moieties and SAPFH.

From the slopes of Mo(VI) adsorbed vs Br^- desorbed (Fig. 5), it can be shown that 34.5 % of the adsorption of Mo(VI) was due to ion exchange corresponding to the acceptance of $HMoO_4^-$. Neutral H_2MoO_4 is the major species and this species may be weakly held by the nonpolar alkyl chain of the surfactant moiety by partition mechanism. Both adsorbent and molybdenum are reproduced and make the process economical.

Impact of association time and initial Mo(VI) concentration

In the case of MoO_4^{2-}, the adsorbed quantity increases from 1.69 to 5.87 mg/g, as the initial concentration is increased from 20 to 100 mg/L and the steady time for 20,
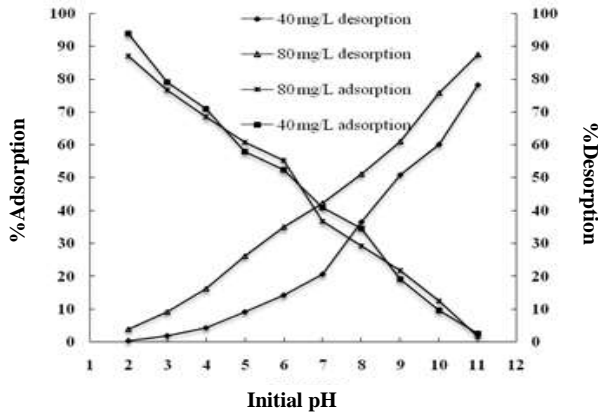
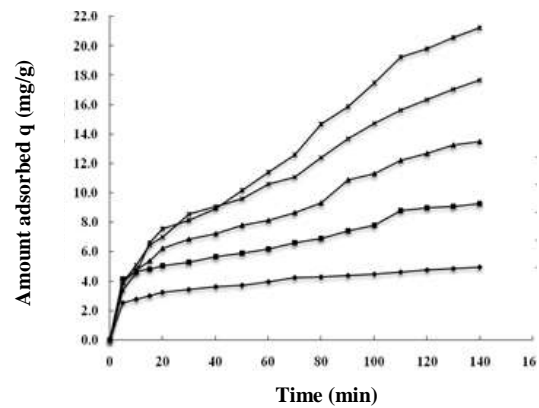**Fig. 4: Impact of pH on the adsorption and desorption of Mo(VI).**

Fig. 6: Effect of agitation time on the adsorption of Mo(VI) onto SAPFH.
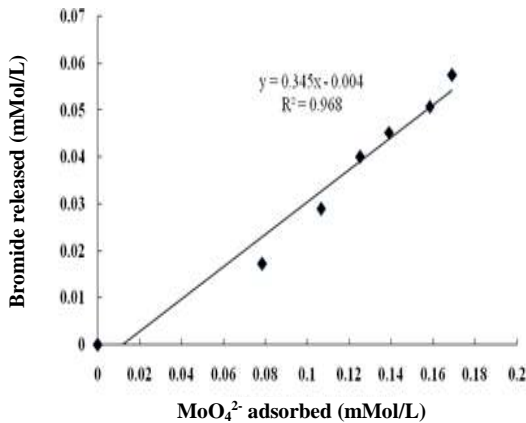

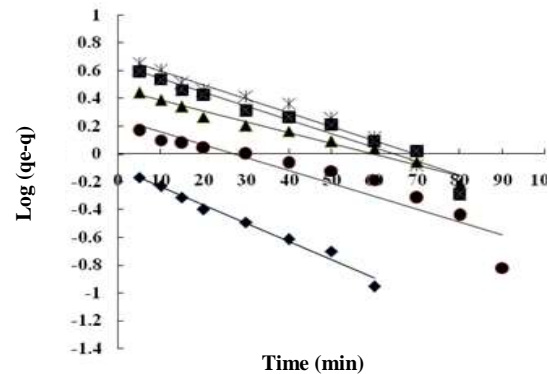**Fig. 5: MoO_4^{2-} uptake and Br release from SAPFH.**

Fig. 8: Second pseudo-order kinetic plots for adsorption of MoO_4^{2-}.

40, 60, 80, and 100 mg/L were 70, 100, 90, 90, and 80 min respectively (Fig. 6). The adsorption of inorganic anions increases over time. Initially, adsorption was rapid due to the presence of more active sites and, after a while, the repellent forces between bulk state and adsorbate molecules on the adsorbent reduce the frequency of filling the remaining vacant surface sites and ultimately, as a result of a deficit in the operative sites the sorption rate become saturated [48]. MoO_4^{2-} took a long time to attain equilibrium at high concentrations.

Adsorption kinetic studies

The adsorption kinetics model is a major aspect in executing the water/wastewater operation technique by coordinating the rate of adsorption of adsorbate with the massive aggregation of the sorbate. To check the rate-determining step, Lagergren pseudo-first order and

pseudo-second order equations were utilized for the dynamic statistics model.

Pseudo First order kinetic model:

Lagergren (1898) explained the pseudo-first-order equation for liquid/solid sorption depending on solid readiness [49], which is a mostly employed uptake rate equation for the uptake of adsorbate from a deliquescent solution.

$$\log(q_e - q) = \log q_e - \frac{k_1 t}{2.303} \qquad (1)$$

Where q_e is the quantity of Mo(VI) uptake (mg/g) at stability time and q is the quantity of Molybdenum ion uptake (mg/g) at duration t, and k_1 is pseudo first order adsorption pace invariable(1/min). Log (q_e-q) vs t graph (Fig. 7) provided the q_e and k_1 values which are exhibited in Table 4 for Mo(VI) ion of varying concentrations.

Table 4: Comparison of the pseudo first and pseudo second order kinetic models for the adsorption of Mo(VI) at 32 °C.

Anion	Initial conc. (mg/L)	q_e (exp) (mg/g)	Pseudo First - order kinetics			Pseudo Second - order kinetics		
			k_1 (1/min)	q_e (cal) (mg/g)	R^2	k_2 (g/mg/min)	q_e (cal) (mg/g)	R^2
MoO_4^{2-}	20	1.6889	-0.030	0.7870	0.981	0.035	2.0806	0.99
	40	3.1212	-0.021	1.7973	0.883	0.0104	4.0358	0.946
	60	4.3500	-0.016	2.8120	0.981	0.0043	6.2650	0.92
	80	5.4727	-0.022	4.3786	0.948	0.0026	8.5360	0.924
	100	5.8696	-0.023	5.0128	0.961	0.0012	11.7581	0.86

* Conditions: Temperature, 32 °C; Adsorbent dose, 0.05 g 50mL⁻¹; pH 2.0

Pseudo Second-order kinetic model:

The pseudo-second-order kinetics is estimated by the following relation [50,51] :

$$\frac{t}{q} = \frac{1}{k_2 q_e^2} + \frac{t}{q_e} \tag{2}$$

Where k_2 is the pseudo-second-order pace invariable (g/mg/min). Graph plotted between t/q vs t (Fig. 8) provides an assessment of q_e and k_2 which are exhibited in Table 4 for Mo(VI) ion of varying concentrations.

The empirical q_e assessments were compared with those estimated in pseudo-first and pseudo-second order dynamic logic. Table 4 shows that q_e assess evaluated in the pseudo-first-order model habitually disagrees with empirical q_e values. A high correlating value is obtained for q_e that is experimentally calculated, and gave satisfactory consent with the q_e values estimated in the pseudo-second-order dynamic logic. Therefore, the uptake of Mo(VI) usually resulted in a pseudo-second-order kinetic model. For the pseudo-second-order kinetic model, the pace invariable generally decreased with increment in the initial adsorbate association for the adsorbate which confirmed the equilibrium time increased with a higher concentration of molybdenum suggesting that the adsorption mechanism followed chemisorptions for rate determining step [52]. A similar outcome showed up for surfactant-modified coir pith [53], $ZnCl_2$ activated carbon [54], sepiolite [55], $ZnCl_2$-activated coir pith carbon [56], and graphene [57].

Adsorption isotherms

The surface assimilation isotherm of Mo (VI) was constructed to determine the uptake ability. The linear equation of the Langmuir isotherm model [58] for the Mo (VI) uptake is evinced as

$$Ce/q_e = 1/Q_0 b + Ce/Q_0 \tag{3}$$

Where C_e is the association of molybdenum ion (mg/L) at balanced state Q_0 invariable representing uptake ability (mg/g) is exhibited in Fig. 9. The chart was linear. The Q_0 and b values are determined from gradient and intercept and are exhibited in Table 5.

The Freundlich isotherm equation for the adsorbate uptake is expressed as [59] (*Freundlich* 1906):

$$\log q_e = \log k_f + \frac{1}{n} \log C_e \tag{4}$$

Where k_f and n are Freundlich isotherm invariable that comprehends the aspects changing the uptake process such as adsorption ability and adsorption magnitude.

Freundlich isotherm is exhibited in Fig. 9. Assess of k_f and *n* are determined from the intercept and gradient of the linear chart of log q_e vs log C_e and are shown in Table 5.

The larger value of k_f shows the high capacity for adsorption. The experimental n values for the anion studied are greater than 1, therefore there are attractive forces between the different adsorbed species [60]. In the present investigation, the calculated n values are $1 < n < 10$ which denotes favorable adsorption for the studied adsorbate [61].

The linear equation of the Dubinin Raduskevich isotherm model for the Mo(VI) uptake is expressed [62] as:

$$\ln q_e = \ln qm - B\varepsilon^2 \tag{5}$$

Where *B* indicates an invariable relating the average free energy uptake per mole of the adsorbate (mol^2/J^2), q_m is the theoretical saturation ability (mol/g) and ε refers the Polanyi potential, which is computed from the relation

$$\varepsilon = RT\ln (1 + 1/Ce) \tag{6}$$

Table 5: Adsorption isotherm constants for the adsorption of inorganic anions at 32 ºC.

An ions	Langmuir			Freundlich			Dubinin - Radushkevich		
	Q_0 (mg/g)	b (L/mg)	R^2	k_f ($mg^{1-1/n}$ $L^{1/n}$ /g)	n	R^2	q_m X 10^3 (mol/ g)	-β×10^9 mol^2/J^2	R^2
MoO_4^{2-}	7.59	0.0866	0.993	1.01	1.99	0.977	1.122×10^{-8}	4.31	0.986
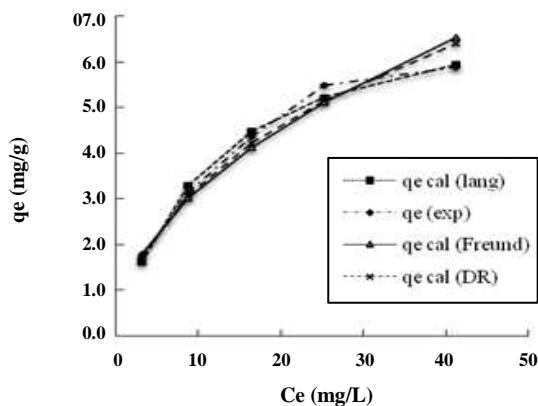
Fig. 9: Adsorption isotherms for MoO_4^{2-}.

Fig. 10: Effect of agitation time and temperature on adsorption of MoO_4^{2-}.

Where R (J mol/K) is gas invariable and T(K) represents the absolute temperature. The chart of ln q_e vs ε^2 provides the gradient and intercept from which the q_m and B assessments were evaluated and given in Table 5.
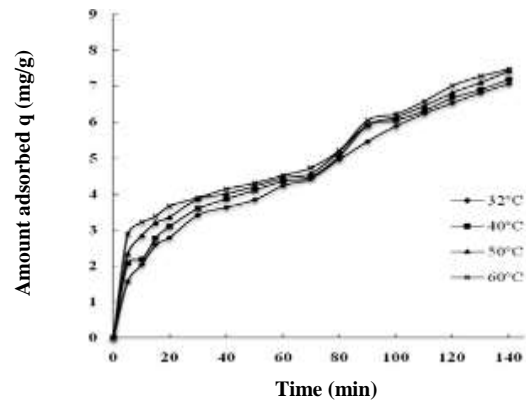
All three isotherms were well suited to the empirical details (Fig. 9). The uptake ability of the Dubinin Raduskevich isotherm is superior to another isotherm. This variance in uptake ability is explained in detail of the inference arrived in the derivation of these adsorption isotherm logics [63]. The regression coefficient values are in the range, 0.97 to 0.99 for all the three isotherms for the adsorbate which depicts that monolayer adsorption as well as the divergent assertive disposition of active sites on the exterior of the surface altered material are attainable for the anion.

The ability of Mo(VI) uptake is maximal at acidic pH 2 by virtue of the positive surface of the surface-altered PFH. A similar report was found in the literature [27, 33].

Impact of temperature

The outcome evinced that there was no symbolic alteration in the uptook quantity (q_e (exp) was around 6.06 mg/g) with temperature rise.

By changing the temperature from 32 to 60 ºC, the amount of adsorbed adsorbate (q_e) vs the time curve (Fig. 10) showed

that the adsorption of adsorbates (q_e values) did not change significantly with an increase in temperature. Identical results were shown in Mo removal by freshly precipitated nascent Mn_3O_4 [64]. This shows that the binding between the adsorbates and SAPFH is of a physical/ion exchange nature. At 32 ⁰C, the ΔG⁰ value was -42.9 kJ/mol, which denoted that the progress took place spontaneously.

Influence of Coexisting Anions

Table 6 shows the adsorption capacity of SAPFH for MoO_4^{2-} in the presence of anions such as Cl^-, SO_4^{2-}, CrO_4^{2-} and PO_4^{3-}. The coexisting negative ions decreased the adsorption capacity as their association elevated from 10-200 mg/L. CrO_4^{2-} and Cl^- compete more with MoO_4^{2-} at all concentrations studied, whereas SO_4^{2-} and PO_4^{3-} ions do not intervene with the MoO_4^2 uptake. The competitive ions have minimized the uptake ability of MoO_4^{2-} in the order $CrO_4^{2-} > Cl^- > SO_4^{2-} > PO_4^{3-}$.

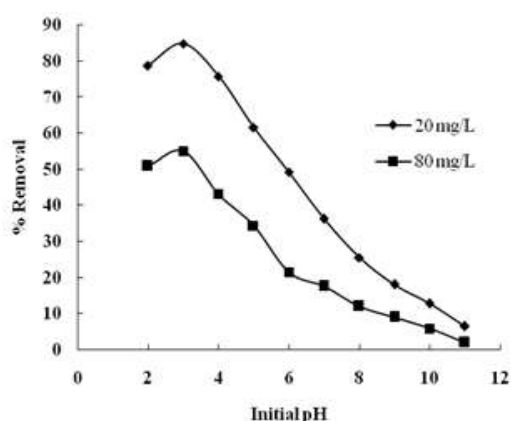### Synthetic wastewater treatment
Effect of pH

Fig.11 shows the maximal extraction of 85 and 55 % respectively, at pH 3.0, for 20 and 80 mg/L MoO_4^{2-} concentrations respectively, in the simulated wastewater is on par with 79% and 77 % respectively, in deliquescent

Table 6: Effect of concentration of coexisting anion on the removal of MoO_4^{2-}.

Foreign ions added	Adsorption capacity (mg/g)			
	10 mg/L	50 mg/L	100 mg/L	200 mg/L
MoO_4^{2-}	16.9			
Cl^-	12.1	11.03	9.34	8.04
PO_4^{3-}	16.3	15.5	14.8	14.0
SO_4^{2-}	15.7	14.5	12.8	12.3
CrO_4^{2-}	10.92	8.85	7.98	5.92

Concentration of MoO_4^{2-}: 20 mg/L   Adsorbent dose : 200 mg/50 mL   Initial pH: 2.0

Fig. 11: Effect of pH on the removal of MoO_4^{2-} from synthetic wastewater.

Fig. 12: Effect of adsorbent quantity on the removal of MoO_4^{2-} from synthetic wastewater.
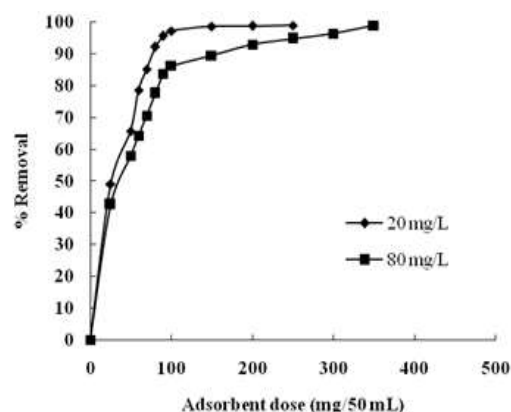
MoO_4^{2-} solutions. At pH 11.0, the removal of about 6 % of MoO_4^{2-} was achieved in synthetic wastewater and the removal was less than 3% for a pure aqueous solution due to the formation of hydroxides of Fe^{3+}, Al^{3+}, and Ca^{2+} whereas these metal hydroxides function as adsorbents for the removing MoO_4^{2-} from synthetic wastewater. In general, basic pH does not favor the removal of anions.

Impact of adsorbent quantity

Fig. 12 depicted the quantitative uptake of MoO_4^{2-} in synthetic wastewater at an adsorbent quantity of 250 mg/50 mL for the MoO_4^{2-} concentrations of 20 and 80 mg/L, respectively whereas in pure aqueous MoO_4^{2-} solutions an adsorbent quantity of 500 mg/50 mL is required for quantitative removal. The adsorbent dose essential for the maximal uptake of MoO_4^{2-} was lesser for the wastewater compared to pure aqueous solutions.

CONCLUSIONS

The biosorbent's surface was changed using cetyltrimethylammonium bromide. The modified palm fruit husk removed Mo(VI) ions successfully from the aqueous solution. The maximal removal of molybdenum occurs at pH 2.0. The adsorbent dose necessary for the maximum adsorption of MoO_4^{2-} was lesser for wastewater than for pure aqueous solutions. MoO_4^{2-} took a long time to attain equilibrium at high concentrations. Equilibrium data of adsorption obeys Langmuir, Freundlich, and Dubinin Raduskevich isotherms. The adsorption systems generally observed pseudo-second-order dynamics for the adsorbate and the uptake mechanism follows ion exchange. The adsorption process becomes economical due to the detachment of the anion from the spent adsorbent. The competitive anions such as Cl^-, SO_4^{2-}, PO_4^{3-}, and CrO_4^{2-} reduced Mo(VI) adsorption capacity.

Abbreviations

PFH	Palm Fruit Husk
SAPFH	Surface Altered Palm Fruit Husk
q_e	Quantity of adsorbate uptook at balanced pace mg/g
k_1	Pseudo First order adsorption pace invariable, min⁻¹
k_2	Pseudo Second order adsorption pace invariable, g/mg .min
C_0	Adsorbate association initially, mg/L
C_e	Association of adsorbate at balanced pace, mg/L
Q_0	Langmuir uptake ability, mg/g

REFERENCES

[1] Rutkowska B., Szulc W., Spychaj-Fabisiak E., Pior N., Prediction of Molybdenum Availability to Plants in Differentiated Soil Conditions, *Plant Soil Environ.,* **63(11)**: 491-497 (2017).

[2] Fujita T., Dodbiba G., Sadaki J., Shibayama A., Removal of Anionic Metal Ions from wastewater by Hydroxide-Type Adsorbents, *Chin. J. Process Eng.,* **(3)**: 357-362 (2006).

[3] WHO, "Guidelines for Drinking -Water Quality", 4th ed., World Health Organization, Geneva (2011).

[4] Namasivayam C., Sureshkumar M.V., Removal and Recovery of Molybdenum from Aqueous Solutions by Adsorption onto Surfactant Modified Coir Pith, A Lignocellulosic Polymer, *Clean- Soil, Air. Water.,* **379**: 60-66 (2009).

[5] Nägler Th.F., Vögelin A.R., Neubert N., Greber N.D., Villa I.M., "Mo Isotope Fractionation in Surface Processes: An Unwanted Complication (Unpublished)." In: *Environmental Isotopes EMI 13.* Ascona. 18-23 August (2013).

[6] Verbinnen B., Block C., Lievens P., Brecht A.V., Vandecasteele C., Simultaneous Removal of Molybdenum, Antimony and Selenium Oxynions from Waste water by Adsorption on Supported Magnetite, *Waste Biomass Valori.,* **4**: 635-645 (2013).

[7] Chao L., Wang Y., Cao Y., Li Y., Adsorption of Molybdenum (VI) in Contaminated Water Using Fe₃O₄/CTS Magnetic Nanoparticles., *E3S Web of Conferences,* **165**, 05032 (2020).

[8] Ting J., Yang-yang J., Shu-juan Y., Ying-ming Q., Zhi-ling J., Yan-hui C., Guo W., Pollution of Molybdenum and Heavy Metals of the Soils and Rice near a Molybdenum Mining Site in Eastern Fujian, *Environmental Monitoring in China.,* **31**(1): 45-49 (2015). (In Chinese)

[9] Kuchekar S.R, Dhage P.M., Aher H.R., Han S.H., Removal of Molybdenum (VI) Using Tamarindous Indica Seeds as a Natural Ion Exchanger, *J. Mater. Environ Sci.,* **11(12)**: 2074-2083 (2020).

[10] WHO. "Guidelines for Drinking - Water Quality", pp.410 (2006).

[11] Orrego P., Jose H., Reyes A., Uranium and Molybdenum Recovery from Copper Leaching Solutions Using Ion Exchange, *Hydrometallurgy,* **184**: 116-122 (2019).

[12] Talla R.G., Gaikwad S.U., Pawar. S.D., Solvent Extraction and Separation of Mo(VI and W(VI) from Hydrochloric Acid Solutions Using Cyanex-923 as Extractants, *Indian J. Chem. Technol.,* **17**(6): 436-440 (2010).

[13] Pradhan D., Kim D.J., Sukla L.B., Pattanaik A., Lee S.W., Evaluation of Molybdenum Recovery from Sulfur Removed Spent Catalyst Using Leaching and Solvent Extraction, *Sci. Rep.,* **10(1)**: 1-14 (2020).

[14] Zhang X., Ma J., Lu X., Huangfu X., Zou J., High Efficient Removal of Trace Molybdenum from Water by FeCl₃, Effects of pH and Affecting Factors in the Presence of Co-Existing Background Constituents, *J. Harbin Inst. Technol.,* **23(4)**:75-83.(2016).

[15] Sabullah M.K., Rahman M.F., Ahmad S.A., Sulaiman M.R., Shukor M.S.A, Shamaan N.A., Shukor M.Y., Assessing Resistance and Bioremediation Ability of Enterobacter Sp. Strain Saw-1 on Molybdenum in Various Heavy Metals and Pesticides, *J. Math. Fundam. Sci,* **49(2)**:193-210 (2017).

[16] Nguyen T.H., Lee M.S., Recovery of Molybdenum and Vanadium with High Purity from Sulfuric Acid Leach Solution of Spent Hydrodesulfurization Catalysts by Ion Exchange, *Hydrometallurgy,***147-148**: 142-147 (2014).

[17] Velizarov S., Crespo J.G., Reis M.A., Removal of Inorganic Anions from Drinking Water Supplies by Membrane Bio/Processes, *Rev. Environ. Sci. BioTechnol.,* **3**: 361-380 (2004).

[18] Yobilishetty S. M., Marathe K.V., Removal of Molybdenum (VI) from Effluent Waste Water Streams by Cross Flow Micellar Enhanced Ultrafiltration (MEUF) Using Anionic, Non-Ionic and Mixed Surfactants, *Indian J. Chem. Technol.,* **2**: 321-327 (2014).

[19] Ferreira S.L.C., Andrade H.M.C., dos Santos H.C., Characterization and Determination of the Thermodynamic and Kinetic Properties of the Adsorption of The Molybdenum (VI) - Calmagite Complex onto Active Carbon, *J. Coll. Interf. Sci.,* **270(2)**: 276-280 (2004).

[20] Xu N., Christodoulatos C., Braida W., Adsorption of Molybdate and Tetrathiomolybdate onto Pyrite and Goethite: Effect of pH and Competitive Anions, *Chemosphere,* **62**: 1726-1735 (2006).

[21] Afkhami A., Norooz-Asl R.., Removal, Preconcentration and Determination of Mo(VI) from Water and Wastewater Samples Using Maghemite Nanoparticles, *Colloids Surf., A. Physicochem. Eng. Asp.,* **346(1-3)**: 52-57 (2009).

[22] Goldberg S., Competitive Adsorption of Molybdenum in the Presence of Phosphorus or Sulfur on Gibbsite, *Soil Sci.,* **175(3)**: 105-110 (2010).

[23] Pennesi C., Totti C., Beoichini F., Removal of Vanadium (III) and Molybdenum(V) from Wastewater Using Posidonia Oceanic (Tracheophyta) Biomass, *PLoS One,* **8(10:e76870):** 1-11 (2013).

[24] Johansson C.L., Paul N.A., Rocky de Nys., Roberts D.A., Simultaneous Biosorption of Selenium, Arsenic and Molybdenum with Modified Algal – Based Biochars, *J. Environ. Manage.,* **165**:117-123 (2016).

[25] Polowczyk I., Cyganowski P., Bruno F Urbano., Bernabe L Rivas., Bryjak M., Kabay N., Amberlite IRA-400 and IRA-743 Chelating Resins for the Sorption and Recovery of Molybdenum(VI) and Vanadium(V): Equilibrium and Kinetic Studies, *Hydrometallurgy,* **169**: 496-507 (2017).

[26] Lian J.J., Huang Y.G., Chen B., Wang S.S., Wang P., Niu S.P., Liu Z.L., Removal of Molybdenum(VI) from Aqueous Solution Using Nano-Zero Valent Iron Supported on Biochar Enhanced by Cetyl-Trimethyl Ammonium Bromide: Adsorption Kinetic, Isotherm and Mechanism Studies, *Water Sci. Technol.,* **2017(3)**: 859-868 (2018).

[27] Denkova A.G., Terpstra B.E., Steinbach O.M., ten Dam J., Wolterbeek H.Th., Adsorption of Molybdenum on Mesoporous Aluminium Oxides for Potential Application In Nuclear Medicine, *Sep. Sci. Technol.,* **48**: 1331-1338 (2013).

[28] Chen Y.C., Lu C., Kinetics, Thermodynamics and Regeneration of Molybdenum Adsorption in Aqueous Solutions with NaOCl-Oxidized Multiwalled Carbon Nanotubes, *J. Ind. Eng. Chem.,* **20(4)**: 2521-2527 (2014).

[29] Sbai S., Elyahyaoui A., Sbai Y., Bentayeb F., Brich M.R., Study of Adsorption Of Molybdate Ion by Alumina, *J. Environ. Res. Develop.,* **11(3)**: 452-460 (2017).

[30] Ito T., Kim S.Y., Adsorption and Separation Behaviors of Molybdenum from High-Level Liquid Waste Using a Silica-Based Hydroxyoxime Impregnated Adsorbent, *J. Radioanal. Nucl. Chem.,* **316**: 1165-1172 (2018).

[31] Ogata F., Nakamura T., Kawasaki N., Adsorption Capability of Virgin and Calcined Wheat Bran for Molybdenum Present in Aqueous Solution and Elucidating the Adsorption Mechanism by Adsorption Isotherms, Kinetics and Regeneration, *J. Environ. Chem. Eng.*, **6(4)**: 4459-4466 (2018).

[32] Brion-Roby R., Gagnon J., Nosrati S., Deschênes J., Chabot B., Adsorption and Desorption of Molybdenum (VI) in Contaminated Water Using a Chitosan Sorbent, *J. Water Process. Eng.,* **23**: 13-19 (2018).

[33] Lian J., Yang, M, Wang. S, Chen, B, Zhou F, Liu Z., Treatment of Molybdenum(VI)- Containing Groundwater Using Chitosan Nanoparticle: Adsorption Mechanism and Performances, *Desalin. Water Treat.*, **167**: 258-268 (2019).

[34] Lian J., Zhou F., Chen B., Yang M., Wang S., Liu Z., Niu S., Enhanced Adsorption of Molybdenum(VI) onto Drinking Water Treatment Residues Modified by Thermal Treatment and Acid Activation, *J. Clean. Prod.,* **244**: 118719 (2020).

[35] Chowdhury Z.Z., Zain S. M., Khan R.A., Rafique R.F., Khalid K., Batch and Fixed Bed Adsorption Studies of Lead(II) Cations from Aqueous Solutions onto Granular Activated Carbon Derived From Mangostana Garcinia Shell, *Bioresources,* **7(3)**: 2895-2915 (2012a).

[36] Chowdhury Z.Z., Zain S.M., Khan R.A., Islam S. Md., Preparation and Characterizations of Activated Carbon from Kenaf Fiber for Equilibrium Adsorption Studies of Copper from Waste Water, *Korean J. Chem. Eng.,* **29(9)**: 1187-1195 (2012b).

[37] Sud D., Mahajan G., Kaur M.P., Agricultural Waste Material as Potential Adsorbent for Sequestering Heavy Metal Ions from Aqueous Solutions-A Review, *Bioresour. Technol.,* **99**:6017-6027 (2008).

[38] Bermejo-Barrera P., Vazquez-Gonzalez J.F., Pazos-Naveira M.C., Bermejo-Martinez F., Determination of Molybdenum with Gallic Acid and Hydroxylamine, *Analyst.,* **112(4)**: 477-479 (1987)

[39] Baird R.B., Eaton A.D., Rice E.W., "Standard Methods for the Examination of Water and Wastewater", 23rd ed., *American Public Health Association, American Water Works Association and Water Pollution Control Federation*, Washington DC (2017)

[40] Sudhakara P., Reddy K.O., Prasad C.V., Jagadeesh D., Kim H.S., Kim B.S., Bae S.I., Song J.I., Studies on Borassus Fruit Fiber and Its Composites with Polypropylene, *Composites Research*, **26**: 48–53 (2013).

[41] Bingol A., Ucun H., Bayhan Y.K., Karagunduz A., Cakici A., Keskinler B., Removal of Chromate Anions from Aqueous Stream by a Cationic Surfactant-Modified Yeast, *Bioresour. Technol.,* **94**: 245-249 (2004).

[42] Krishna B.S., Murty D.S.R., Jaiprakash B.S., Thermodynamics of Chromium (VI) Anionic Species Sorption onto Surfactant-Modified Montmorillonite Clay, *J. Coll. Interf. Sci.,* **229(1)**: 230-236 (2000).

[43] Arami M., Limaee N.Y., Mahmoodi N.M., Tabrizi N.S., Removal of Dyes from Colored Textile Wastewater by Orange Peel Adsorbent: Equilibrium and Kinetic Studies, *J. Coll. Interf. Sci.,* **288(2)**: 371-376 (2005).

[44] Kreller D.I., Gibson G., vanLoon G.W., Horton J.H., Chemical Force Microscopy Investigation of Phosphate Adsorption on the Surfaces of Iron(III) Oxyhydroxide Particles, *J. Coll. Interf. Sci.,* **254(2)**: 205-213 (2002).

[45] Egute N.S., Sousa J.S., Yamaura M., Study on Removal of Molybdenum From Aqueous Solution Using Sugarcane Bagasse ash as Adsorbent, *International Nuclear Atlantic Conference. Nuclear Energy: New Jobs for a Better Life-INAC* 2011, October 24-28, Belo Horizonte, MG, Brazil (2011).

[46] Gustafsson J.P., Modelling Molybdate and Tungstate Adsorption to Ferrihydrite, *Chem. Geol.,* **200(1-2)**: 105-115 (2003).

[47] Bostick B.C., Fendorf S., Helz G.R., Differential Adsorption of Molybdate and Tetrathiomolybdate on Pyrite (FeS$_2$), *Environ. Sci. Technol.,* **37(2)**: 285-291 (2003).

[48] Sulyman M., Namiesnik J., Gierak A., Low-Cost Adsorbents Derived from Agricultural by-Products/Wastes for Enhancing Contaminant Uptakes from Wastewater: A Review, *Pol. J. Environ. Stud.,* **26**: 479-510 (2017).

[49] Lagergren S., Zur Theorie Der Sogenannten Adsorption Gelöester Stoffe (in German), Kungliga Svenska Vetenskapsa-Kademiens, *Handlingar.,* **24**: 1-39 (1898)

[50] Blanchard G., Maunaye M., Martin G., Removal of Heavy Metals from Waters by Means of Natural Zeolites, *Water Res.,* **18(12)**: 1501-1507 (1984).

[51] Ho Y.S., Mckay G., Sorption of Dye from Aqueous Solution by Peat, *Chem. Eng. J.* **70(2)**: 115 –124 (1998).

[52] Yamaura M., Santos J.L., Damasceno M.O., Egute N.S., Moraes A.A.N., Santos B.Z., "Biomass as Biosorbent for Molybdenum Ions", *International Nuclear Atlantic Conference-INAC* 2013, November 24-29, Brazil (2013).

[53] Namasivayam C., Sureshkumar M.V., Surfactant Modified Coir Pith, an Agricultural Solid Waste as Adsorbent for Phosphate Removal and Fertilizer Carrier to Control Phosphate Release, *J. Environ. Sci. Eng.,* **47**(4): 256- 265 (2005).

[54] Namasivayam C., Sangeetha D., Removal and Recovery of Vanadium (V) by Adsorption onto ZnCl$_2$ Activated Carbon: Kinetics and Isotherms, *Adsorption,* **12**: 103-117 (2006).

[55] Öztürk N., Bektas T. E., Nitrate Removal from Aqueous Solution by Adsorption onto Various Materials, *J. Hazard. Mater.,* **112**: 155-162 (2004).

[56] Namasivayam C., Sangeetha D., Application of Coconutcoir Pith for the Removal of Sulphate and Other Anions from Water, *Desalination,* **219(1-3)**: 1–13 (2008).

[57] Ganesan P., Kamaraj R., Vasudevan S., Application of Isotherm, Kinetic and Thermodynamic Models for the Adsorption of Nitrate Ions on Graphene from Aqueous Solution, *J. Taiwan Inst. Chem. E.*, **44(5)**: 808-814 (2013).

Research Article

[58] Langmuir I., The Adsorption of Gases on Plane Surfaces of Glass, Mica and Platinum, *J. Amer. Chem. Soc.,* **40(9)**: 1361-1403 (1918).

[59] Freundlich H.M.F., Uber Die Adsorption in Losungen, *Z. Phys. Chem.,* **57A**: 385 (1906).

[60] Ramachandran J., Vivekanandan S., Lakshmi S., Adsorption Behaviour of N-haloarene Sulphonamidates on Activated Carbon at 303 K, *Indian J. Chem.,* **40A**: 115-118 (2001).

[61] McKay G., Otterburn M.S., Sweeney A.G., The Removal of Colour from Effluent Using Various Adsorbents- III. Silica: Rate Processes, *Water Res.,* **14**(1): 15-20 (1980).

[62] Özcan A.S., Erdem B., Özcan A., Adsorption of Acid Blue 193 from Aqueous Solutions onto BTMA-Bentonite, *Colloids Surf., A. Physicochem. Eng. Asp.,* **266(1-3)**: 73-81 (2005).

[63] Hasany S.M., Saeed M.M., Ahmed M., Sorption of Traces of Silver Ions onto Polyurethane Foam from Acidic Solution, *Talanta.,* **54(1)**: 89-98 (2001).

[64] Zhao Z., Liu J., Xia W., Cao C., Chen X., Huo G., Chen A., Li H., Removal of Molybdenum from Mnso4 Solution with Freshly Precipitated Nascent Mn_3O_4, *Hydrometallurgy,* **99(1-2)**: 67-71 (2009).